Egyptian Journal of Aquatic Biology & Fisheries
Zoology Department, Faculty of Science,
Ain Shams University, Cairo, Egypt.
ISSN 1110 – 6131
Vol. 28(6): 1145 – 1159 (2024)
www.ejabf.journals.ekb.eg

Nineteen Years Temporal of Seagrass Change and Carbon Stock in Jepara Region Indonesia

Sigit Febrianto[1]*, Max Rudolf Muskananfola[1], Suryanti Suryanti[1], Nurul Latifah[1], Hadi Endrawati[2]

[1]Department of Resource Aquatic, Faculty of Fisheries and Marine Science, Diponegoro University, Indonesia

[2]Department of Marine Science, Faculty of Fisheries and Marine Science, Diponegoro University, Indonesia

***Corresponding Author: febriantosigit40@gmail.com**

ARTICLE INFO

Article History:
Received: Aug. 30, 2023
Accepted: Oct. 26, 2024
Online: Dec. 4, 2024

Keywords:
Carbon stock,
Seagrass bed,
Mapping,
Climate change,
Jepara

ABSTRACT

Seagrass is a coastal ecosystem that plays a role in absorbing CO_2 and mitigating climate change. At Bandengan Beach in Jepara Regency, there has been no time-series monitoring of seagrass changes for the past 19 years, creating a data gap. This study aimed to assess the ability of seagrass to absorb CO_2 and store organic carbon (Corg) as well as to examine the temporal changes in seagrass beds at Bandengan Beach from 2001 to 2020. A combination of remote sensing and field survey methods was used in this research. Carbon content was calculated using the Loss On Ignition (LOI) method, while seagrass cover and biomass mapping were analyzed using the Lyzenga and supervized classification methods. Three seagrass species were identified: *Cymodocea serrulata*, *Thalassia hemprichii*, and *Enhalus acaroides*. The seagrass area decreased by 1.4 ha (68%), from 2.05 ha in 2001 to 0.64 ha in 2020. The highest density (663 individuals per m²) and the highest biomass (481.28 g DW per m²) were dominated by *C. serrulata*, which also exhibited the highest carbon stock potential: 16.42 gC per m² above ground (AGB), 22.17 gC per m² below ground (BGB), and a total carbon stock of 4.21 tons per hectare. Based on this research, the preservation of seagrass ecosystems, which play a crucial role in mitigating climate change through CO_2 absorption, is essential.

INTRODUCTION

Seagrass beds are coastal ecosystems that have the ability to absorb and store CO_2 in both tissue biomass and sediment, with amounts approximately 3 to 5 times greater than those of land vegetation. As a result, they contribute to coastal blue carbon, alongside mangrove and peat swamp ecosystems **(Pendleton *et al.*, 2012; Mazarrasa *et al.*, 2018)**. In addition to the absorption of CO_2, the seagrass plant has an important role in the water ecosystem since it has high productivity, functions as a sediment trap, and plays a role in supporting the life of aquatic organisms through its ecological function and bioindicators of coastal health **(Lovelock & Reef, 2020; Lambert *et al.*, 2021; Ghallab *et al.*, 2022)**. One of the areas in Central Java where the seagrass ecosystem is still quite good is in the Jepara waters. Carbon sequestration by Indonesia's seagrasses was estimated to be 5.62–8.40 ton C ha^{-1} yr^{-1} **(Wahyudi *et al*., 2020)**. This is greater than the CO_2 absorption capacity of tropical forests over the same area **(Phinn *et al*., 2008; Fourqurean *et al.*, 2012)**.

In recent decades, there has been a decrease in seagrass area due to human activities, especially coastal development and land conversion, thus affecting the carbon cycle and the potential of CO_2 absorbed by blue carbon. This has resulted in a decrease in seagrass area and the threat of seagull habitat in the International Union for the Conservation of Nature (IUCN) protection category **(Macreadie *et al*., 2014; Abo Elenin *et al.*, 2020; Jones *et al*., 2020)**. The Government of Indonesia, through Presidential Decree No. 61 of 2011, committed to reducing greenhouse gas emissions by regulating activities in five sectors, namely agriculture, forestry, peatland, energy, transport, industry and waste management **(Vaughn *et al*., 2021)**. According to **Alongi *et al*. (2016)**, Indonesia's mangrove and seagrass ecosystems hold 17% of the world's carbon reserves. The estimation of carbon seagrass global baseline is in the range of 4.2 Pg and 4.8 (C_{org}) carbon organic Pg **(Shrestha *et al.*, 2019; Zeller *et al*., 2021)**.

Research on seagrasses is still mainly conducted in Europe, America **(Hoa *et al.*, 2019; Islam *et al*., 2022)**, Australia and parts of Asia such as Vietnam, the Philippines, Thailand, Malaysia **(Poursanidis *et al*., 2019; Dahiru *et al.*, 2022)**. In Indonesia, however, it is still limited on the potential of carbon sequestration and has not studied the dynamics of changes in the area of seagrass meadows over a long period of time. The aim of this study was to examine the trend changes in the seagrass area and estimated carbon stock over 19 years at Bandengan Beach. The problem with blue carbon in Indonesia is the lack of complete baseline data on the ecosystem conditions in which blue carbon occurs. The combination of remote sensing and blue carbon is a solution to this problem because remote sensing can analyze changes in the area over a long period of time, combined with the results of field measurements of carbon uptake. The findings of this research would benefit as a reference for conservation and coastal management.

MATERIALS AND METHODS

1. Study area and data sources

The study was conducted in October 2018 at Bandengan Beach Jepara, Central Java, using three lines of sampling points with a distance of 5 metres between points (Fig 1). Seasonally, this study area of Jepara waters, as part of the Java Seas, consists of west and east monsoonal and transitional seasons, with the west and east seasons tending to have rough seas (higher waves) than transitional seasons **(Muskananfola *et al.*, 2020; Muskananfola *et al*., 2023)**. At each point, aboveground, belowground, and sediment carbon measurements were taken for comparison. The materials used in this study were seagrass samples and sediments collected from the water of the beach. Landsat 7 ETM, Landsat 8 OLI and Sentinel 2A, 2B satellite imagery data were used to analyze seagrass biomass, cover, and carbon content (Table 1).

Table 1. Research data

No	Satellite data	Year	Source
1	Landsat 7 TM	2001	Earth Explore
2	Landsat 8 OLI	2014	Earth Explore
3	Sentinel 2A, 2B	2018, 2020	ESA Copernicus
4	Google Earth	2001,2014,2018,2020	https://www.google.co.id/intl/id/earth/

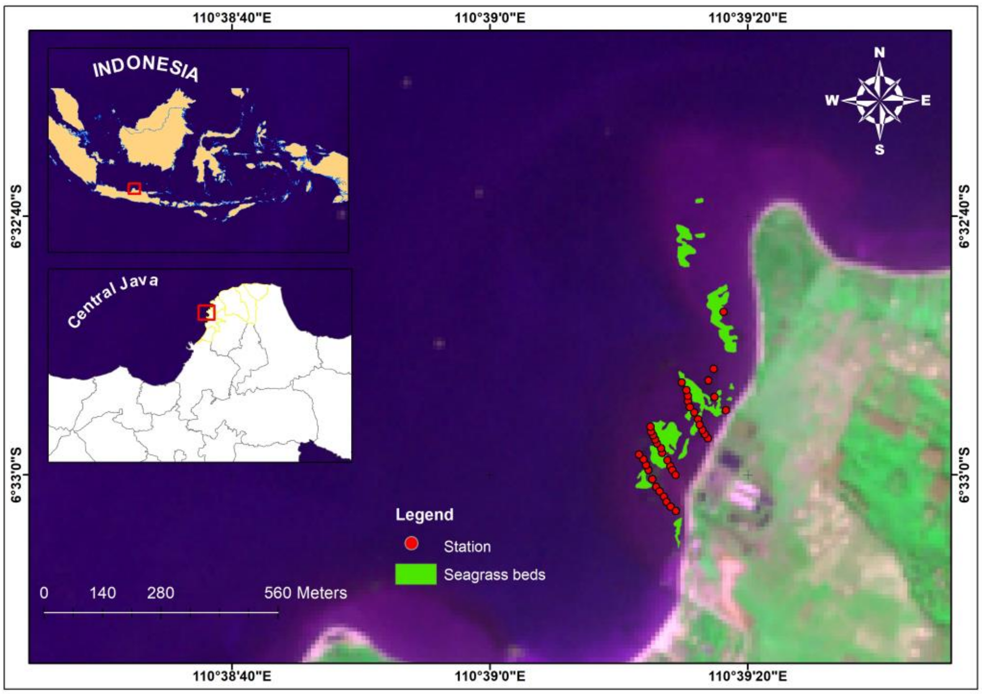

Fig. 1. Map research location

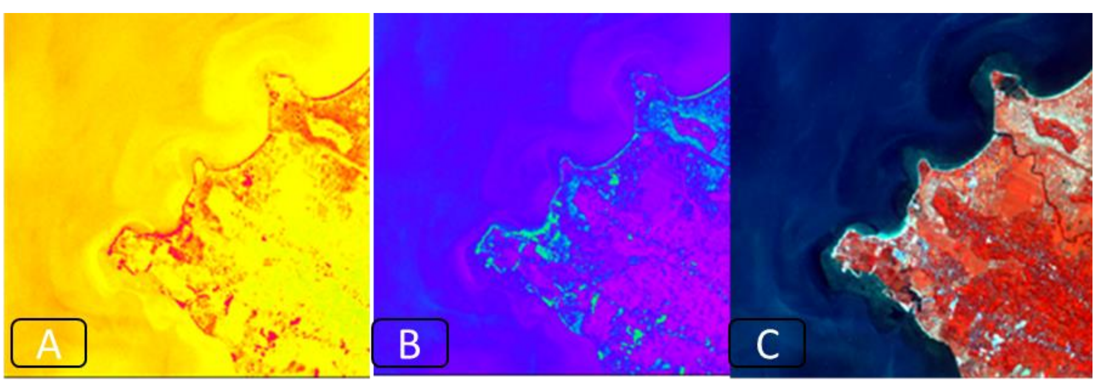

Fig. 2. Processing Sentinel 2A satellite image **a)** Before radiometric correction; **b)** Radiometric correction; and **c)** RGB composite

The seagrass samples were taken up to 10 stands. This was done by sampling seagrass down to the roots in quadrant transects. This is done to be valid and to represent the biomass sample of each observation point **(Hartati *et al.*, 2017)**. Seagrass plants are divided into three (3) parts, namely leaves, rhizomes and roots.

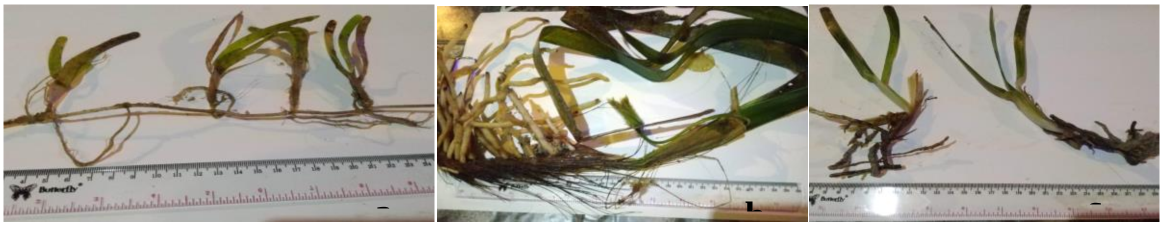

Fig. 3. Main seagrass species at Bandengan Beach: **a)** *C. Serrulata*; **b)** *E. Acoroides*; and **c)** *T. Hemprichi*

2. Image analysis

In this study, all satellite image data from 2001 to 2020 (Fig. 2) were atmospherically corrected using Dark Object Subtraction via the Semi-Automatic Classification plugin in QGIS **(QGIS Development Team, 2019; Congedo, 2021)**. Digital numbers were converted to reflectance values for the blue, green, red, NIR, and SWIR spectral bands. Changes in seagrass area were then analyzed (Fig. 2). The Lyzenga algorithm for water column correction was applied to all satellite images **(Lyzenga, 1981; Hedley *et al.*, 2012)**. The water attenuation mapping formula using the Lyzenga algorithm is described below.

$$Y = \ln TM1 + {}^{k_i}\!/_{k_j} \ln TM2 \quad (1)$$

$$ {}^{k_i}\!/_{k_j} = a + \sqrt{\left(a^2+1\right)}$$

$$a = \frac{\left(\mathrm{var}\, TM1 - \mathrm{var}\, TM2\right)}{2 * \mathrm{cov}ar TM1TM2}$$

The calculation of the algorithm is influenced by the pairs of bands i (blue) and j (green), as used by **Lyzenga (1981)**, with the blue and green bands having the best penetration among other bands. In Landsat satellite images, the blue and green spectral bands correspond to bands 1 and 2, respectively, while in Sentinel-2 images, they correspond to bands 2 and 3. Supervised classification using maximum likelihood and support vector machine methods was applied to classify the images into four categories: sand, dead coral, seagrass, and mud. For classification, 80 training areas were used as reference data, evenly distributed across the study area.

3. Organic carbon storage

Organic carbon samples were taken from seagrass separated between leaves and rhizome stems. The carbon content of seagrass was calculated using the Loss on Ignition

(LOI) method, which was carried out at the Livestock Nutrition Laboratory, Universitas Diponegoro. The calculation of carbon values was done for all seagrass species found in the transect frame **(Hulopi *et al*., 2017)**. The value of carbon concentration obtained from seagrass biomass of the same species was used as a benchmark to convert the seagrass biomass into a carbon content value (e.g. 100 grams of seagrass produces 1 gram of carbon, or carbon biomass = 1/100 biomass seagrass). Total carbon stocks were calculated using the method of **Fourqurean *et al.* (2012)** and **Hartati *et al*. (2017)**. Organic carbon storage (C_{org}) within the seagrass beds was calculated:

Total C_{org} = A * (C_{org} in living biomass + C_{org} in sediment) (2)

Carbon loss = % rate of change in seagrass * Δ Total C_{org} (3)

Where, A is the seagrass cover (ha), while C_{org} in living biomass and C_{org} in sediment **(Stankovic *et al*. 2018)**. CO_2 emissions associated with the change in seagrass bed cover were calculated as follows:

CO_2 emissions = (Total C_{org} subsequent assessment – Total C_{org} initial assessment)* 3.67 (4)

Where, the total initial C_{org} and total subsequent C_{org} assessments represent the values of C_{org} loss between years. A conversion factor of 3.67 is used to convert C_{org} to CO_2.

Seagrass biomass

The seagrass biomass was calculated using the formula of **Duarte (1990)**

B = W X D (5)

Where :

B = Biomass (dry) Seagrass (gr dry/m); W= Dry weight (gr/stands); D = Seagrass density (stands/m^2)

Carbon seagrass

Carbon content in seagrass tissues was calculated using the equation of **Helrich (1990)**:

Ash content = $c-a/b-a$ x 100% (6)

Organic materials were calculated by weight reduction during a raid **(Helrich, 1990)**:

Organic matter = $[(b-a)(c-a)]/(b-a)$ x 100% (7)

Where, a = weight of the cup, B = weight of the cup + dry weight of the seagrass tissue, C = weight of the cup + ash weight of the seagrass network.

After the process of phishing, organic material was converted into biomass:

Carbon = Organic material content/1.724 (8)

Where:

1.724 = constant value of organic material **(Helrich, 1990)**.

RESULTS

1. Seagrass abundance

Three species of seagrass dominate the waters of Bandengan: *Thalasia hemprichi*, *Cymodocea serrulata*, and *Enhalus acoroides* (Fig 3). Table (2) shows the density and distribution of seagrass species in the study area.

Table 2. Seagrass cover and density in Bandengan Beach Jepara

No	Species	Seagrass density (ind m^{-2})			% cover		
		line 1	line 2	line 3	line 1	line 2	line 3
1	*Thalasia hemprichi*	26	58.67	118.28	45	32.5	33.57
2	*Cymodocea serrulata*	344.12	164.5	82.5	54.23	40.83	30.83
3	*Enhalus acoroide*	0	3	0	0	5	0

The results in Table (2) indicates that the distribution and density of seagrass beds are randomly scattered at each point in each line where the highest density is located on line 1 with a density of 344 ind m^{-2}, and seagrass covers 54.23% dominated by the species *Cymodocea serrulata*, while the lowest density dominated by the species *Enhalus acoroides* which is scattered on all lines. Line one is located near the outlet of the shrimp hatchery and agriculture. There are several reasons for the uneven distribution of seagrass species at each site, one of which is the bottom substrate. The seagrass species *Enhalus acoroides* thrives on sand substrates mixed with mud, while the seagrass species *Cymodocea serrulata* and *Thalasia hemprichi* have bottom substrate preferences of mud-sand and coral fragments.

2. Dynamics changes of seagrass meadow

Each plot was sampled in 33 quadrant plots, each consisting of 3 line transects. Data collected included percent cover, species identification, cover density, and sediment samples. The results are presented using satellite images for the seagrass area from 2001 to 2020, while 2018 field data were used to validate seagrass percentage cover, density, and carbon stock. In 2001, the seagrass area was 2.05 ha. Over the next 13 years (2001–2014) (Fig. 4), the seagrass cover decreased significantly by 55%, reducing the area to 0.99 ha (Table 2). From 2014 to 2018, there was a very significant increase in seagrass area of 84%, bringing the area up to 1.68 ha (Fig. 4). However, in the subsequent 2 years (2018–2020), the seagrass area decreased by 61%, resulting in a final area of 0.64 ha.

Based on the analysis of the dynamics of seagrass, area changes are divided into 3 categories, namely no change with yellow color, new with green color and loss with red color. There was no change in the dynamic area in the years 2001–2014, which remained at 0.21 ha. In the years 2014–2018, the dynamic area increased by 0.52 ha, while from 2018 to 2020, the dynamic area decreased by 0.51 ha. The new dynamic area in 2001–

2014 was 0.69 ha, in 2014–2018 was 1.16 ha, and in 2018–2020 was 0.13 ha. The loss of dynamic area in 2001–2014 was 1.85 ha, in 2014–2018 was 0.9 ha, and in 2018–2020 was 1.17 ha (Fig. 5).

Changes in the seagrass area over nineteen years (2001–2020) are shown in Fig. (5). Significant changes occurred in the seagrass area, with a loss of 0.2 ha, a new area of 0.44 ha, and a loss of 1.85 ha from the total area of 2.05 ha in 2001. Table (3) illustrates the direct effect of these changes on total C_{org}, carbon loss, and CO_2 release. Total C_{org} decreased from 5.49 MgC ha–1 in 2001 to 1.71 MgC ha–1 in 2020, with a total carbon loss of 5.17 MgC ha–1 over the 19-year period. This resulted in a total CO_2 emission of 13.86 $MgCO_2$ during the same period.

Fluctuations in land use changes affecting carbon loss were influenced by the transformation of Bandengan Beach into tourist areas, residential areas, fishing boat docks, and shrimp hatcheries. From 2001 to 2020, land cover change fluctuated, with a decrease of 0.55 to 0.61 hectares, indicated by the red areas. In 2018, land cover increased significantly by 0.87 hectares, shown in green, while the yellow areas remained unchanged (Fig. 5).

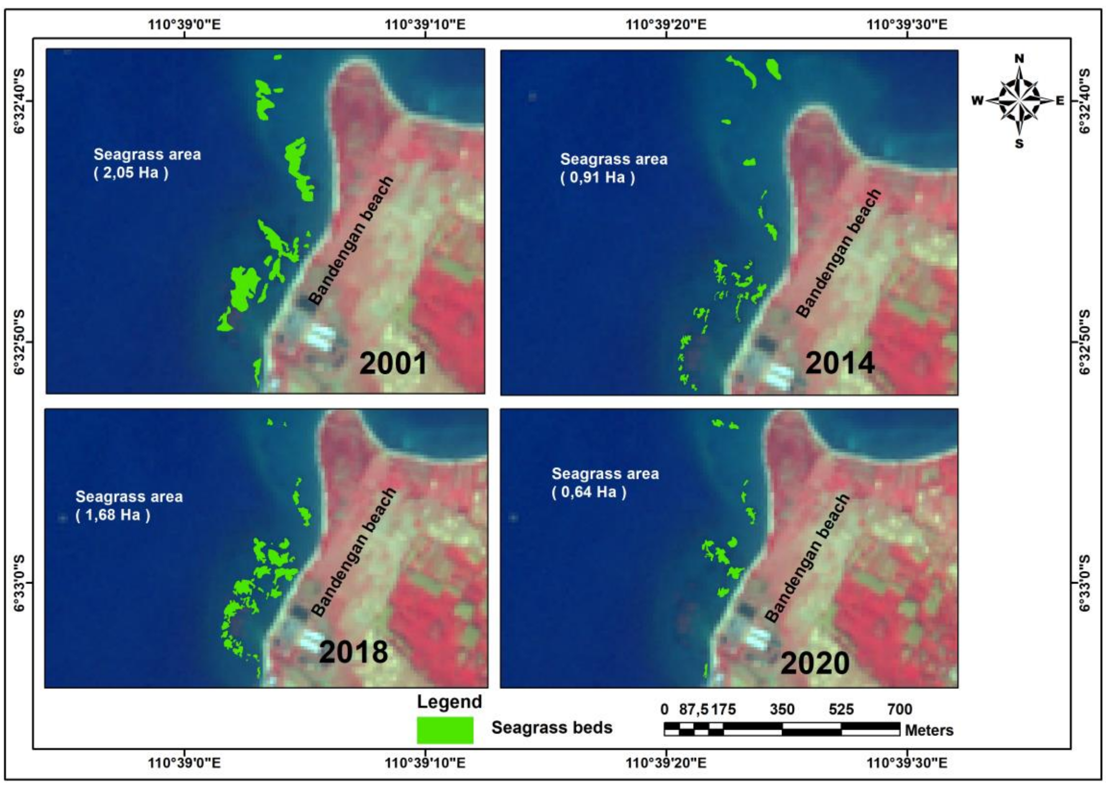

Fig. 4. Seagrass bed distribution at Bandengan Beach across 19 years 2001, 2014, 2018, and 2020

Table 3. Change rates of seagrass beds from 2001-2020

Year	Area (ha)	% rate of change in seagrass	Total C_{org} (Mg C/ha)	Carbon loss (Mg C/ha)	CO_2 emission ($MgCO_2$/yr)
2001	2.05	-	5.49	-	-
2014	0.91	-0.55	2.43	1.68	-11.21
2018	1.68	+0.87	4.50	1.79	+7.57
2020	0.64	-0.61	1.71	1.70	-10.22
Total		**-0.29**	**14.15**	**5.17**	**-13.86**

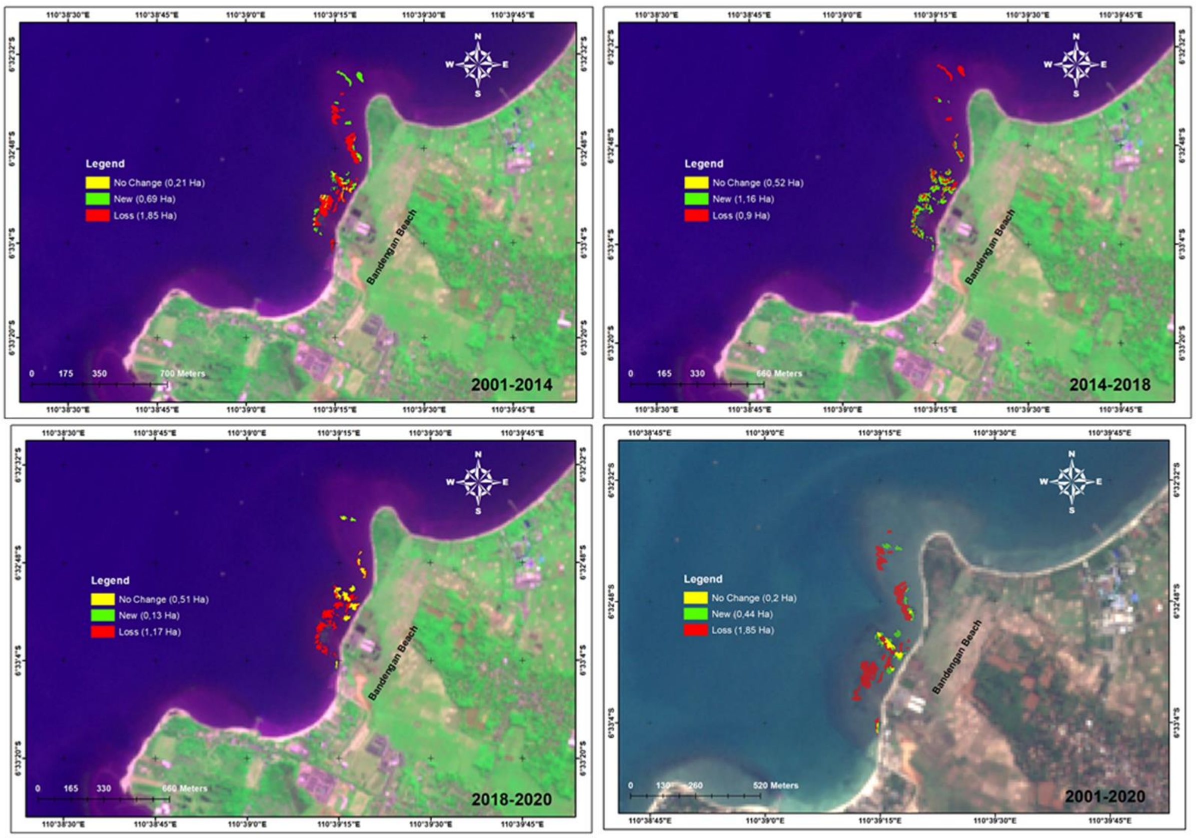

Fig. 5. Seagrass area change between 2001–2020

3. Seagrass beds carbon stock

Based on the analysis of the carbon sequestration estimation, the seagrass beds in Bandengan Beach Jepara have carbon stocks of 4.21 ton ha^{-1} in the form of continuous seagrass, while in the form of patchy seagrass beds, the carbon stocks ranged between 1.45 and 1.48 ton ha^{-1} (Table 2). Bandengan Beach has medium to high turbidity and the meadow type is continuous to patchy. The values of above-ground biomass and below-ground biomass show that above-ground values ranged from 5.68 to 16.42 gC m^{-2}, and below-ground values ranged from 8.83 to 22.17 gC m^{-2}. Table (2) shows that the below-ground biomass (BGB) is 30% higher than the above-ground biomass (AGB). The type of seagrass meadow, whether continuous or patchy, also affects the amount of AGB and BGB stored, as well as the total carbon stock in seagrass biomass.

Table 2. Seagrass beds carbon storage in Jepara

Site	Sample	n	Seagrass cover	Meadow type	Turbidity level	AGB (gC m^{-2})	BGB (gC m^{-2})	Total Stock Carbon (ton/ha)
Bandengan beach 1	Seagrass beds	9	48	Continuous	medium	16.42	22.17	4.21
Bandengan beach 2	Seagrass beds	13	24	Patchy	high	5.45	9.37	1.48
Bandengan beach 3	Seagrass beds	13	25	Patchy	medium	5.68	8.83	1.45

DISCUSSION

During the period 2001–2020, seagrasses in Bandengan Beach experienced a significant annual decrease in area and carbon sequestration of up to 29%, and there was an annual increase in the area of 10%, higher than the global estimate of 0.4-2.6% **(Macreadie *et al*., 2014; Almahasheer *et al.*, 2017; Wicaksono *et al*., 2022)** due to land conversion and environmental changes. At Bandengan Beach, three seagrass species were found, dominated by *Thalasia hemprichi, Cymodocea serrulata, Enhalus acoroides*. The seagrass with the highest density is *C. serrulata* 344.12 ind. m^{-2} with a cover of 54%, which is in the moderate category. This condition is higher compared to the same location in 2018 and is generally representative of seagrass density and cover across Indonesia **(Duarte Moreno *et al.*, 2021; Fauzan *et al*., 2021; Wahyudi *et al*., 2022)**. The dominance and density of seagrass beds are strongly influenced by substrate type and meadow type of seagrass. *C. serrulata* is often found in bed type of clay-sand substrate mixed with coral fragments, while *E. acoroides* are often found in muddy-sand substrates **(Ghallab *et al*., 2022; Heng *et al*., 2022)**.

Based on spatial analysis of seagrass meadow changes using multi-temporal satellite imagery, as shown in studies by **Nehren and Wicaksono (2018)** and **Sudo *et al.* (2021)**, Fig. (4) illustrates two types of seagrass meadows, patchy and continuous. It also highlights different substrate types, such as sand, silty sand, and clay mixed with coral fragments. In general, anthropogenic influences, in the form of land use changes, have both direct and indirect effects on the decline of seagrass beds. Tourist developments, settlements, fishing ports, and shrimp hatcheries have contributed to changes in seagrass ecosystems, particularly during the period from 2001 to 2014, when seagrass coverage significantly decreased by 55%. Additionally, natural influences, such as the phenology of seagrass beds, have also played a role **(McKenzie, 2003; Collier *et al*., 2021)**. In 2014 and 2018, seagrass area increased by 0.87 ha, which was the highest increase in area, due to the non-operation of cultivation and hatchery areas and the formation of a clumped seagrass bed type, which allows seagrass beds to be stronger when hit by higher waves in the west and east seasons **(Chen *et al*., 2016; Jayanthi *et al*., 2018; Nguyen *et al*., 2022)**. The carbon storage of the seagrass beds at Bandengan Beach has the highest carbon stock of 4.21 ton/ha and the lowest of 1.45 ton/ha with a seagrass area of 1.68 ha. The high carbon stock is due to the type of substrate in the form of coral fragments containing calcium carbonate, although the seagrass area is small, yet it has a high ability to carbon stock, which is consistent with research results of **Trejo *et al*. (2016)**. **Macreadie *et al*. (2019)** elucidated that blue carbon stocks, especially seagrasses, are at their highest in sediments and above ground. High and low aboveground and belowground carbon stocks are influenced by several main factors such as seagrass species, seagrass meadow type and substrate, with large seagrasses such as *T hemprichi*, *E acaroides* and *C. serrulata* having higher aboveground and belowground contents than other seagrasses due to differences in leaf, stem and rhizome size **(Lovelock & Reef, 2020; Trevathan-Tackett *et al*., 2021)**.

CONCLUSION

The results showed that below-ground carbon storage is 30–45% higher than above-ground storage. This can be explained by the fact that, in the calculation, the stem and rhizome are considered part of the below-ground biomass, while above-ground biomass only includes the leaves, resulting in different sample weights. Seagrass meadows are significant contributors to C_{org} and carbon stocks, and conservation efforts should adopt multidisciplinary approaches, incorporating both ecological studies and remote sensing, to obtain comprehensive information and time-series data.

CrediT authorship contribution statement

All authors are considered primary contributors. SF: Conceptualization, Methodology, Software analysis, Writing—review and editing; HE, SYT: Data curation, field data analysis, and result interpretation; MRM and NL: Writing—review and editing, Supervision.

Declaration of competing interest

The authors declare that they have no known competing financial interests or personal relationships that could have appeared to influence the work reported in this paper.

Acknowledgements

The authors would like to thank Universitas Diponegoro, Jacob Rais Street, Semarang City, Indonesia, for the research grant under the RPP Scheme 753-03/UN7.D2/PP/IX/2022. They also express gratitude to the UNDIP PSDIL FPIK Laboratory, UNDIP Animal Nutrition Laboratory, and Sigit Blue Carbon Laboratory for their assistance with data analysis.

REFERENCES

Abo Elenin, A.H.; Saber, S.A.; El-Kafrawy, S. B. and El-Naggar, H.A. (2020). An integrated field survey and remote sensing approach for marine habitat mapping along Hurghada Coast Red Sea. Egypt. Aquat. Biol. Fish., 24(7): 287–306.

Almahasheer, H.; Serrano, O.; Duarte, C.M.; Arias-Ortiz, A.; Masque, P. and Irigoien, X. (2017). Low carbon sink capacity of Red Sea mangroves. Sci. Rep., 7: 1–10.

Alongi, D. M.; Murdiyarso, D.; Fourqurean, J.W.; Kauffman, J.B.; Hutahaean, A.; Crooks, S.; Lovelock, C. E.; Howard, J.; Herr, D.; Fortes, M.; Pidgeon, E. and Wagey, T. (2016). Indonesia's blue carbon: a globally significant and vulnerable sink for seagrass and mangrove carbon. Wetl. Ecol. Manag., 24(1): 3–13.

Chen, C.F.; Lau, V.K.; Chang, N.; Bin, Son, N.T.; Tong, P.H.S. and Chiang, S.H. (2016). Multi-temporal change detection of seagrass beds using integrated Landsat TM/ETM +/OLI imageries in Cam Ranh Bay, Vietnam. Ecol. Inform., 35: 43–54.

Collier, C.J.; Langlois, L.M.; McMahon, K.M.; Udy, J.; Rasheed, M.; Lawrence, E.; Carter, A.B.; Fraser, M.W. and McKenzie, L.J. (2021). What lies beneath: Predicting seagrass below-ground biomass from above-ground biomass, environmental conditions and seagrass community composition. Ecol. Indic., 121: 1–11.

Congedo, L. (2021). Semi-Automatic Classification Plugin: A Python tool for the download and processing of remote sensing images in QGIS. J. Open Source Softw., 6(64): 1–6.

Dahiru, M.Z.; Hashim, M. and Hassan, N. (2022). Sharpening of thermal satellite imagery from klang industrial area in peninsular malaysia using the tsharp approach. Int. Arch. Photogramm. Remote Sens. Spatial Inf. Sci., XLVI-4/W3-2021: 87–102.

Duarte, C.M. (1990). Seagrass Nutrient Content. Mar. Ecol. Prog. 67: 201–207.

Duarte Moreno, H.; Reuter, H.; Kase, A. and Teichberg, M. (2021). Seaweed farming and land-use impacts on seagrass meadows in the region of Rote Island, Indonesia. Estuar. Coast. Shelf Sci., 263: 107635.

Fauzan, M.A.; Wicaksono, P. and Hartono. (2021). Characterizing Derawan seagrass cover change with time-series Sentinel-2 images. Reg. Stud. Mar. Sci., 48: 102048.

Fourqurean, J.W.; Duarte, C.M.; Kennedy, H.; Marbà, N.; Holmer, M.; Mateo, M. A.; Apostolaki, E.T.; Kendrick, G.A.; Krause-Jensen, D.; McGlathery, K.J. and Serrano, O. (2012). Seagrass ecosystems as a globally significant carbon stock. Nat. Geosci., 5(7): 505–509.

Ghallab, A.; Mahdy, A. and Hussein, H.N.M. (2022). Distribution of seagrass communities and associated sea cucumbers in North Red Sea Protectorates, Hurghada. Egypt. Aquat. Biol. Fish., 26(2): 17–29.

Hartati, R.; Pratikto, I. and Pratiwi, T.N. (2017). Biomassa dan Estimasi Simpanan Karbon pada Ekosistem Padang Lamun di Pulau Menjangan Kecil dan Pulau Sintok , Kepulauan Karimunjawa. Bul. Oseanografi Marina., 6(1): 74–81.

Hedley, J. D.; Roelfsema, C.; Koetz, B. and Phinn, S. (2012). Capability of the sentinel 2 mission for tropical coral reef mapping and coral bleaching detection. Remote Sens. Environ. 120: 145–155.

Helrich, K. (1990). Method 988.05. Official Methods of Analysis, 15th Edition, The Association of Official Analytical Chemists Inc., Arlington.

Heng, H.W.K.; Ooi, J.L.S.; Affendi, Y.A.; Kee Alfian, A.A. and Ponnampalam, L.S. (2022). Dugong feeding grounds and spatial feeding patterns in subtidal seagrass: A case study at Sibu Archipelago, Malaysia. Estuar. Coast. Shelf Sci. 264: 107670.

Hoa, P.V.; Giang, N.V.; Binh, N.A.; Hai, L. V. H.; Pham, T.D.; Hasanlou, M. and Bui, D.T. (2019). Soil salinity mapping using SAR Sentinel-1 data and advanced machine learning algorithms: A case study at Ben Tre Province of the Mekong River Delta (Vietnam). Remote Sens., 11(2): 1–21.

Hulopi, M.; Tuahatu, J. W. and Tuhumury, N. C. (2017). Seagrass potency as blue carbon source in Galala and Tanjung Tiram waters, Ambon Island, Indonesia. AACL Bioflux., 10(5): 1019–1025.

Islam, M.M.; Akther, S. M.; Hossain, M. F. and Parveen, Z. (2022). Spatial distribution and ecological risk assessment of potentially toxic metals in the Sundarbans mangrove soils of Bangladesh. Sci. Rep., 12(1): 1–14.

Jayanthi, M.; Thirumurthy, S.; Muralidhar, M. and Ravichandran, P. (2018). Impact of shrimp aquaculture development on important ecosystems in India. Glob. Environ. Chang., 52: 10–21.

Jones, A.R.; Raja Segaran, R.; Clarke, K.D.; Waycott, M.; Goh, W.S.H. and Gillanders, B.M. (2020). Estimating Mangrove Tree Biomass and Carbon Content: A Comparison of Forest Inventory Techniques and Drone Imagery. Front. mar. sci., 6: 1–13.

Lambert, V.; Bainbridge, Z. T.; Collier, C.; Lewis, S. E.; Adams, M. P.; Carter, A.; Saunders, M. I.; Brodie, J.; Turner, R. D. R.; Rasheed, M. A. and O'Brien, K. R. (2021). Connecting targets for catchment sediment loads to ecological outcomes for seagrass using multiple lines of evidence. Mar. Pollut. Bull., 169: 112494.

Lyzenga, D.R. (1981). Remote Sensing of Bottom Reflectance and WaterAttenuation Parameters in Shallow Water Using Aircraft and Landsat Data. Int. J. Remote Sens. 2(1): 71–82.

Lovelock, C. E. and Reef, R. (2020). Variable Impacts of Climate Change on Blue Carbon. One Earth., 3(2): 195–211.

Macreadie, P.I.; Anton, A.; Raven, J.A.; Beaumont, N.; Connolly, R.M.; Friess, D.A.; Kelleway, J.J.; Kennedy, H.; Kuwae, T.; Lavery, P.S.; Lovelock, C.E.; Smale, D.A.; Apostolaki, E.T.; Atwood, T.B.; Baldock, J.; Bianchi, T.S.; Chmura, G.L.; Eyre, B.D.; Fourqurean, J.W.; Hall-Spencer, J.M.; Huxham, M.; Hendriks, I.E.; Krause-Jensen, D.; Laffoley, D.; Luisetti, T.; Marbà, N.; Masque, P.; McGlathery, K.J.; Megonigal, J.P.; Murdiyarso, D.; Russell, B.D.; Santos, R.; Serrano, O.; Silliman, B.R.; Watanabe, K. and Duarte, C.M. (2019). The future of Blue Carbon science. Nat. Commun. 10: 1–13.

Macreadie, P. I.; Baird, M. E.; Trevathan-Tackett, S. M.; Larkum, A. W. D. and Ralph, P.J. (2014). Quantifying and modelling the carbon sequestration capacity of seagrass meadows - A critical assessment. Mar. Pollut. Bull., 83(2): 430–439.

Mazarrasa, I.; Samper-Villarreal, J.; Serrano, O.; Lavery, P. S.; Lovelock, C. E.; Marbà, N.; Duarte, C. M. and Cortés, J. (2018). Habitat characteristics provide insights of carbon storage in seagrass meadows. Mar. Pollut. Bull., 134: 106–117.

McKenzie, L.J. (2003). Guidelines for the rapid assessment and mapping of tropical seagrass habitats. Seagrass-Watch HQ 46.

Muskananfola, M.R.; Supriharyono. and Febrianto, S. (2020). Spatio-temporal analysis of shoreline change along the coast of Sayung Demak, Indonesia using Digital Shoreline Analysis System. Reg. Stud. Mar. Sci., 34: 101060.

Muskananfola, M.R.; Latifah, N.; Hartoko, A.; Febrianto, S. and Winterwerp, J.C. (2023). The Partial Pressure of CO_2 and Fluxes of CO_2 in Semarang Bay, Indonesia. Ilmu Kelaut.: Indones. J. Mar. Sci., 28(1): 113–124.

Nehren, U. and Wicaksono, P. (2018). Mapping soil carbon stocks in an oceanic mangrove ecosystem in Karimunjawa Islands, Indonesia. Estuar. Coast. Shelf Sci., 214: 185–193.

Nguyen, X.V.; Nguyen-Nhat, N.T.; Nguyen, X.T.; Dao, V.H.; McDermid, K.J. and Papenbrock, J. (2022). Microsatellite-based analysis of the genetic diversity and population structure of the seagrass species Thalassia hemprichii from southern Vietnam. Aquat. Bot. 178: 103497.

Pendleton, L.; Donato, D. C.; Murray, B. C.; Crooks, S.; Jenkins, W. A.; Sifleet, S.; Craft, C.; Fourqurean, J. W.; Kauffman, J. B.; Marbà, N.; Megonigal, P.; Pidgeon, E.; Herr, D.; Gordon, D. and Baldera, A. (2012). Estimating Global "Blue Carbon" Emissions from Conversion and Degradation of Vegetated Coastal Ecosystems. PLoS ONE., 7(9): e43542.

Phinn, S.; Roelfsema, C.; Dekker, A.; Brando, V. and Anstee, J. (2008). Mapping seagrass species, cover and biomass in shallow waters: An assessment of satellite multi-spectral and airborne hyper-spectral imaging systems in Moreton Bay (Australia). Remote Sens. Environ., 112(8): 3413–3425.

Poursanidis, D.; Traganos, D.; Reinartz, P. and Chrysoulakis, N. (2019). On the use of Sentinel-2 for coastal habitat mapping and satellite-derived bathymetry estimation using downscaled coastal aerosol band. Int. J. Appl. Earth Obs. Geoinf., 80: 58–70.

QGIS Development Team. (2019). QGIS Geographic Information System. Open Source Geospatial Foundation Project. http://qgis.osgeo.org.

Shrestha, S.; Miranda, I.; Kumar, A.; Pardo, M. L. E.; Dahal, S.; Rashid, T.; Remillard, C. and Mishra, D. R. (2019). Identifying and forecasting potential biophysical risk areas within a tropical mangrove ecosystem using multi-sensor data. Int. J. Appl. Earth Obs. Geoinf., 74: 281–294.

Stankovic, M.; Tantipisanuh, N. and Prathep, A. (2018). Carbon storage in seagrass ecosystems along the Andaman coast of Thailand. Bot. Mar. 61(5): 429–440.

Sudo, K.; Quiros, T.E.A.L.; Prathep, A.; Luong, C.; Van Lin, H.J.; Bujang, J.S.; Ooi, J.L.S.; Fortes, M.D.; Zakaria, M.H.; Yaakub, S.M.; Tan, Y.M.; Huang, X. and Nakaoka, M. (2021). Distribution, Temporal Change, and Conservation Status of Tropical Seagrass Beds in Southeast Asia: 2000–2020. Front. Mar. Sci., 8: 637722.

Trejo, H. H. and Sánchez, D.M. (2016). Estimation of Carbon Stocks from Mexico's Pantanos de Centla Mangroves.

Trevathan-Tackett, S.M.; Kepfer-Rojas, S.; Engelen, A.H.; York, P.H.; Ola, A.; Li, J.; Kelleway, J.J.; Jinks, K.I.; Jackson, E.L.; Adame, M.F.; Pendall, E.; Lovelock, C.E.; Connolly, R.M.; Watson, A.; Visby, I.; Trethowan, A.; Taylor, B.; Roberts, T.N.B.; Petch, J.; Farrington, L.; Djukic, I. and Macreadie, P.I. (2021). Ecosystem type drives tea litter decomposition and associated prokaryotic microbiome communities in freshwater and coastal wetlands at a continental scale. Sci. Total Environ. 782, 146819.

Vaughn, D. R.; Bianchi, T. S.; Shields, M. R.; Kenney, W. F. and Osborne, T. Z. (2021). Blue Carbon Soil Stock Development and Estimates Within Northern Florida Wetlands. Earth Sci. Front., 9: 1–16.

Wahyudi, A.J.; Rahmawati, S.; Irawan, A.; Hadiyanto, H.; Prayudha, B.; Hafizt, M. and Kiswara, W. (2020). Assessing carbon stock and sequestration of the tropical seagrass meadows in Indonesia. Ocean Sci., 55: 85–97.

Wahyudi, A.J.; Hernawan, U.E.; Alifatri, L.O.; Prayudha, B.; Sani, S.Y.; Febriani, F. and Ulumuddin, Y.I. (2022). Carbon-offset potential from tropical seagrass conservation in selected areas of Indonesia. Mar. Pollut. Bull., 178: 113605.

Wicaksono, P.; Maishella, A.; Wahyudi, A.J. and Hafizt, M. (2022). Multitemporal seagrass carbon assimilation and aboveground carbon stock mapping using Sentinel-2 in Labuan Bajo 2019–2020. Remote Sens. Appl. Soc. Environ., 27: 100803.

Zeller, M.; Van Dam, B.; Lopes, C.; Smyth, A.; Böttcher, M.; Osburn, C.; Zimmerman, T.; Pröfrock, D.; Fourqurean, J. and Thomas, H. (2021). When

"Blue Carbon" turns white: Isotopic evidence of calcification-driven CO_2 emissions in a carbonate seagrass meadow. EGU21-4539.